Entropic Barriers in Nanoscale Adhesion Studied by Variable Temperature Chemical Force Microscopy

5 AUTHORS, INCLUDING:

Aleksandr Noy
Lawrence Livermore National Laboratory
133 PUBLICATIONS   **6,620** CITATIONS

SEE PROFILE

Salvador Zepeda
SunEdison
31 PUBLICATIONS   **411** CITATIONS

SEE PROFILE

Christine A. Orme
Lawrence Livermore National Laboratory
101 PUBLICATIONS   **2,625** CITATIONS

SEE PROFILE

Yin Yeh
University of California, Davis
111 PUBLICATIONS   **2,665** CITATIONS

SEE PROFILE

Entropic Barriers in Nanoscale Adhesion Studied by Variable Temperature Chemical Force Microscopy

Aleksandr Noy,*,† Salvador Zepeda,‡ Christine A. Orme,† Yin Yeh,‡ and James J. De Yoreo†

Department of Chemistry and Materials Science, Lawrence Livermore National Laboratory, Livermore, California 94550, and Department of Applied Science, University of California Davis, Davis, California 95616

Received May 10, 2002 ; E-mail: noyl@llnl.gov

Abstract: Intermolecular interactions drive the vast majority of condensed phase phenomena from molecular recognition to protein folding to particle adhesion. Complex energy barriers encountered in these interactions include contributions from van der Waals forces, hydrogen bonding, and solvent medium. With the spectacular exception of hydrophobic interactions, contributions from the medium are usually considered secondary. We report a variable temperature force microscopy study of the interactions between several hydrogen bonds in different solvents that challenges this point of view. Surprisingly, we observed an increase in the strength of the interaction between carboxylic acid groups in ethanol as the temperature increased. Moreover, when we switched to a nonpolar solvent we observed the opposite behavior: The binding force decreased as the temperature increased. Kinetic model of bond dissociation provided quantitative interpretation of our measurements. We attributed the observed phenomena to a large entropic contribution from the ordered solvent layers that are forming on the probe and sample surfaces upon detachment. The observed reversal in the force vs temperature trend is a manifestation of a transition between thermodynamic and kinetic regimes of unbinding predicted by the model. Our results indicate that entropic barriers dominated by the interactions of solvent molecules with the surface exist in a much wider variety of systems than previously thought.

Introduction

Intermolecular interactions are ubiquitous in condensed phase phenomena.[1] In particular, formation and breakage of various chemical bonds determines the outcome of many important processes such as molecular recognition in biological systems, particle adhesion, and interface fracture in solids. Understanding complex chemical and biological systems depends critically on our ability to model the kinetics and thermodynamics of these interactions. Modern ultra-sensitive force detection methods based on atomic force micropy (AFM)[2] and other techniques[3] enabled measurements of single protein–ligand interaction strength,[4,5] chemical-interaction strength[6] and potential-energy profiles.[7,8] We can divide these measurements into two categor-

ies: single bond interactions, typically encountered in biological systems, and surface–surface interactions, that typically arise from large ensembles of bonds. Researchers traditionally use rather different approaches to describe these types of measurements. On one hand, single bond rupture in biological systems is treated as a kinetic problem of an escape over a potential energy barrier under the assistance of an external force.[9] On the other hand, traditional multi-bond AFM adhesion measurements are described using interfacial free energies of the interacting surfaces.[10] The latter description bundles a number of factors such as chemical nature of the surfaces, temperature, and the contributions of the surrounding medium to the energy barrier into a single thermodynamic quantity: interfacial free energy. Traditionally, interaction force measurements (especially AFM-based measurements) focus on investigating different types of surface forces and studying the effects of different surface chemical functionalities,[11] whereas other factors, such as the contributions of the surrounding medium, receive comparatively little attention.[12]

† Department of Chemistry and Materials Science, Lawrence Livermore National Laboratory.
‡ Department of Applied Science, University of California Davis.
* Corresponding author.

(1) Israelachvili, J. *Intermolecular and Surface Forces*; Academic Press: New York, 1992.
(2) Clausen-Schaumann, H.; Seitz, M.; Krautbauer, R.; Gaub, H. E. *Curr. Opin. Chem. Biol.* **2000**, *4*, 524−530.
(3) Evans, E.; Ritchie, K.; Merkel, R. *Biophys. J.* **1995**, *68*, 2580.
(4) Florin, E. L.; Moy, V. T.; Gaub, H. E. *Science* **1994**, *264*, 415−417.
(5) Merkel, R.; Nassoy, P.; Leung, A.; Ritchie, K.; Evans, E. *Nature* **1999**, *397*, 50−53.
(6) Frisbie, C. D.; Rozsnyai, L. F.; Noy, A.; Wrighton, M. S.; Lieber, C. M. *Science* **1994**, *265*, 2071.
(7) Jarvis, S. P.; Yamada, H.; Yamamoto, S. L.; Tokumoto, H.; Pethica, J. B. *Nature* **1996**, *384*, 247−249.

(8) Ashby, P. D.; Chen, L. W.; Lieber, C. M. *J. Am. Chem. Soc.* **2000**, *122*, 9467−9472.
(9) Evans, E.; Ritchie, K. *Biophys. J.* **1997**, *72*, 1541−1555.
(10) Noy, A.; Vezenov, D.; Lieber, C. *Annu. Rev. Mater. Sci.* **1997**, *27*, 381−421.
(11) Noy, A.; Frisbie, C. D.; Rosznyai, L. F.; Wrighton, M. S.; Lieber, C. M. *J. Am. Chem. Soc.* **1995**, *117*, 7943.
(12) Sinniah, S. K.; Steel, A. B.; Miller, C. J.; Reutt-Robey, J. E. *J. Am. Chem. Soc.* **1996**, *118*, 8925−8931.

In this paper, we use temperature dependence of the interaction forces to distinguish among different contributions to the interaction strength. In particular, we focus on the contributions from the surrounding medium. We present a framework for separating the interaction strength into enthalpic, entropic, and kinetic components based on the kinetic model of the bond dissociation.[9,13] We point out the importance of the entropic part of the energy barrier and discuss several possible regimes of force-assisted detachment based on the relative weight of the entropic and kinetic contributions to the interaction strength. We also present a set of variable-temperature chemical force microscopy experiments demonstrating a transition between these regimes.

Experimental Section

Materials and Chemicals. We used commercial silicon nitride AFM probes: NP−S (Digital Instruments/Veeco, Santa Barbara, CA), and Microlevers (ThermoMicroscopes/Veeco, Sunnyvale, CA). Silicon (111) wafers were supplied by Silicon Sense, Nashua, NH. 16-mercapto-hexadecanoic acid and hexadecanethiol were purchased from Aldrich and used as received. To modify the surfaces with well-defined chemical functionalities the AFM probes and silicon wafers were first coated with 50 Å of Ti followed by 1000 Å of gold. We then immersed AFM probes and silicon samples in freshly made 10 mM solutions of the alkanethiol in ethanol for 12 h. The probes and samples were taken out of solution immediately before the experiment. Prior to being mounted in the microscope fluid cell probes and samples were rinsed with ethanol and dried under a filtered nitrogen stream.

Variable Temperature Chemical Force Microscopy. We used a custom-built variable temperature AFM setup based on the Nanoscope II atomic force microscope (Digital Instruments/Veeco, Santa Barbara, CA). Detailed description of the setup is given elsewhere.[14] Briefly, we machined a custom copper sample holder that incorporated an thermoelectric element (Omega Engineering, Stamford, CT). The temperature in the microscope cell was monitored by two thermocouples (immediately above and below the sample) and maintained by PID feedback circuit. The microscope was enclosed in a custom-built two-layer environmental chamber cooled with cold dry nitrogen gas. Nitrogen also prevented water condensation on the microscope optical elements. This setup maintains the temperature in the microscope fluid cell to better than 0.1 °C precision over a wide range of temperatures.

Cantilever Spring Constant Calibration. Large variations in the spring constants of the commercial cantilevers require individual calibration of every cantilever used for quantitative measurements. We calibrated our cantilevers individually over the experimental range of temperatures using the thermal resonance method.[15]

Adhesion Force Measurements and Data Processing. We measured adhesion forces by recording AFM cantilever deflection in the "force curve" cycle. The magnitude of the pull-off jump in the retraction part of the force curve provided the measure of the adhesion force. We kept the loading rate constant at 200 nN/s. The distribution of the pull-off forces is always broadened by the variations in tip−sample contact area and thermal noise. Therefore, to quantify the spread in the binding force values and to obtain a reliable measurement of the pull-off force we recorded multiple force vs distance curves for each temperature point. To minimize the variability associated with the probe shape, we used the same tip−sample combination to study interaction forces in different solvents. AFM probes modified with self-assembled monolayers are susceptible to catastrophic failure of gold coating. Therefore, probe lifetime considerations typically forced us to limit the number of individual force curves to 40 at each temperature point.

When we used more durable Si_3N_4 probes, we increased the number of individual force curves per each temperature point to ~300. We used IgorPro data analysis software (WaveMetrics, Lake Oswego, OR) and a set of custom procedures (courtesy of Dr. D. V. Vezenov) to extract the values of the adhesion force from the force curves. We obtained average values of the pull-off forces by fitting the histograms of the pull-off force distributions to a Gaussian function. For all tip−sample combinations, binding force values were independent of maximum load force applied in the force curve cycle. We obtained similar trends regardless of whether the temperature was raised, lowered, or varied randomly during the experiment.

Results and Discussion

Variable-Temperature Chemical Force Microscopy. To evaluate the energy barriers encountered in intermolecular interactions, we measured adhesion forces between a probe tip of an atomic force microscope and a sample as a function of temperature. For these measurements, we combined chemical force microscopy (CFM) and a novel variable-temperature AFM stage[14] that allows rigorous control over an extended temperature range (Figure 1). CFM is a technique developed by Lieber and co-workers which uses AFM probes modified with specific chemical functional groups to probe specific interactions.[10] We modified the surfaces of the probe and the sample with a thin layer of gold followed by alkanethiol self-assembled monolayer (SAM) terminating in carboxylic acid functional groups. This system allowed us to measure interactions between a number of well-defined hydrogen bonding groups[11] (Figure 1A, inset). Thiol modification provided a robust means of a rigorous control over the chemical functionality of the interacting surfaces. We conducted all our interaction force measurements in fluid environment to get rid of capillary forces that often obscure other types of interactions for AFM measurements in ambient conditions. In addition, we feel that measurements of intermolecular forces should be conducted preferentially in fluid environment because most of the intermolecular interactions relevant for biophysical and interfacial phenomena occur in liquids. Interaction forces measured in the AFM experiments show large variations between individual measurements. Therefore, to quantify these variations and to obtain reliable values of the average pull-off forces we collected multiple force curves for each measurement point and fitted the histograms of the pull-off force to a Gaussian function (Figure 2).

Quantitative chemical force microscopy measurements depend critically on the knowledge of cantilever spring constants. Careful spring constant calibration is particularly important for the variable temperature measurements because any variations in the cantilever spring constant with temperature may distort force vs temperature trends. Ideally, the temperature dependence of a cantilever spring constant is determined by the temperature response of the cantilever material elastic modulus, which is negligible for typical cantilever materials such as silicon and silicon nitride. However, a typical AFM cantilever is coated with a thin reflective metal layer that turns the cantilever to a bimetallic strip and causes it to bend in response to a temperature change.[16] Additional gold coating, which is necessary for chemical modification of the AFM probes, only exacerbates the bending. Unfortunately, this bending also changes the effective cantilever

(13) Bell, G. I. *Science* **1978**, *200*, 618−627.
(14) Zepeda, S.; Yeh, Y.; Orme, C. A. *Rev. Sci. Instr.* **2001**, *72*, 4159−4163.
(15) Hutter, J. L.; Bechhoefer, J. *Rev. Sci. Instr.* **1993**, *64*, 1868−1873.

(16) Barnes, J. R.; Stephenson, R. J.; Woodburn, C. N.; Oshea, S. J.; Welland, M. E.; Rayment, T.; Gimzewski, J. K.; Gerber, C. *Rev. Sci. Instr.* **1994**, *65*, 3793−3798.
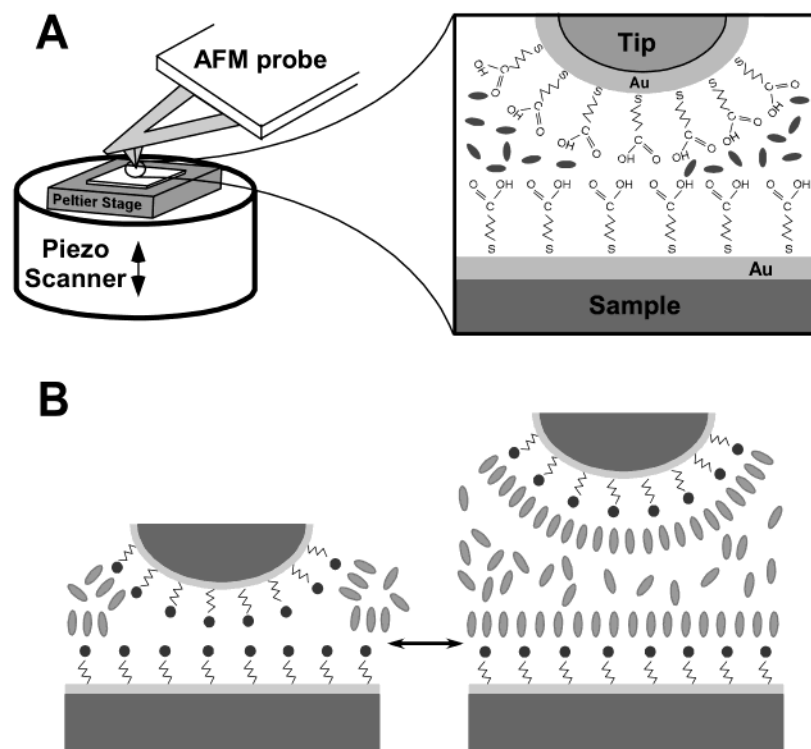
Figure 1. (A). Schematics of the temperature controlled AFM used for the experiments. (**Inset**) A cartoon showing interactions between a tip and the sample modified with self-assembled monolayers terminated with carboxylic acid functional groups. (B) A cartoon illustrating formation of the ordered solvent layers during the transition from the bound state (left) to the unbound state (right).
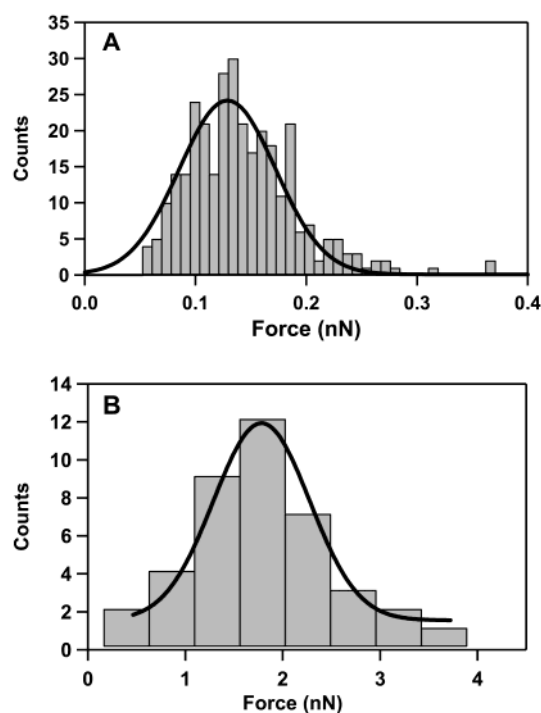
Figure 2. (A) Histogram of binding force values obtained for Si_3N_4 tip and mica sample in ethanol at 0 °C. The histogram contains data from 300 individual force vs distance measurements. Solid line represents a Gaussian fit to the data. (B) Histogram of binding force values obtained for COOH-terminated tip and sample in ethanol at −6.6 °C. The histogram contains data from 40 individual force vs distance measurements. Solid line represents a Gaussian fit to the data.

geometry and internal stress, which can lead to variations in the spring constant with temperature. To account for these effects, we always calibrated our cantilevers individually using
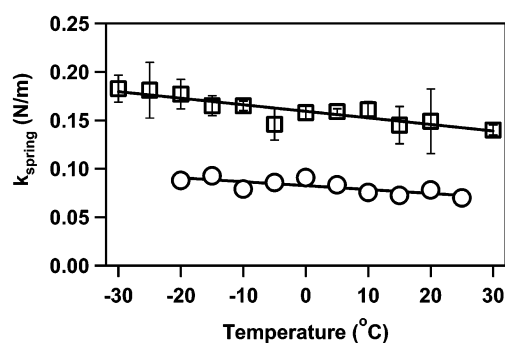

Figure 3. Typical plot of the measured spring constant as a function of temperature for gold-coated AFM cantilevers: 200 μm long model NP−S cantilever (○) and a 220 μm long Microlever D cantilever (□). The error bars on the top dataset (□) correspond to uncertainties from 10 individual calibration procedures performed at each temperature point.

thermal resonance method[15] at different points over the temperature range that we studied. We typically observed that the spring constant for our gold-coated cantilevers decreased as the temperature increased with the total decrease up to ~35% over the 40 °C range (Figure 3). This trend was consistent for all cantilevers that we used.

To evaluate the energy barriers between hydrogen-bonding chemical functionalities we measured interaction forces between probe and sample surfaces terminated with carboxylic acid functional groups. Intuitively, we expected the chemical bond strength to decrease at higher temperatures as the bonds "loosen up" due to increased thermal fluctuations of the molecules involved in the interaction. When we measured the adhesion force between these surfaces in hexane, we indeed observed a decrease in the adhesion force with temperature (Figure 4A). However, when we switched the solvent to ethanol, not only
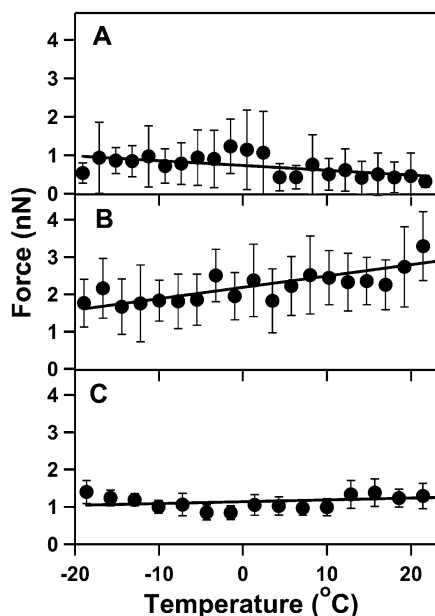
Figure 4. Plots of measured adhesion force as a function of temperature for COOH-terminated tip and sample in (A) hexane, (B) ethanol, and (C) 1:1 ethanol:hexane mixture. Each data point corresponds to an average of 40 individual force vs distance curves.
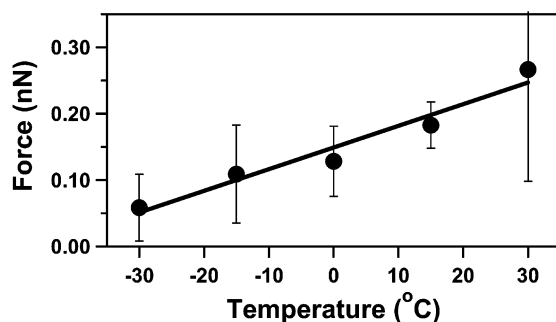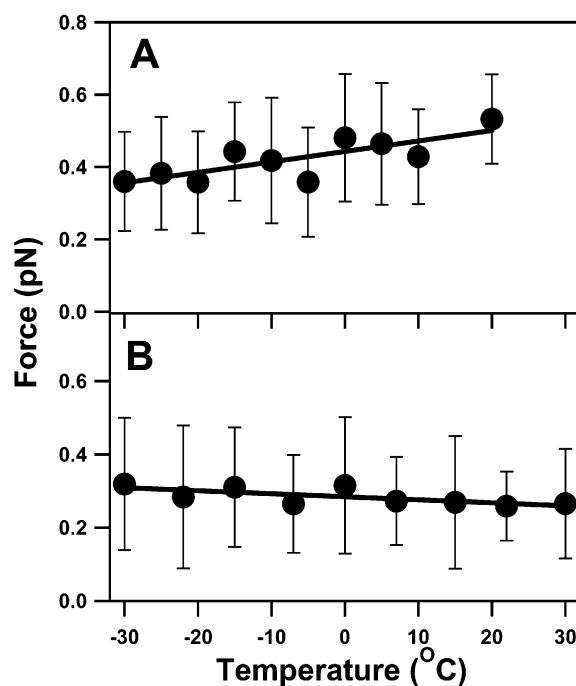

Figure 5. Plot of measured adhesion force as a function of temperature for Si_3N_4 tip and mica surface. Each data point corresponds to an average of 300 individual force vs distance curves.

did we measured an adhesion force that was stronger than the adhesion force measured in hexane, but also we observed a surprising increase in the adhesion force as the temperature increased (Figure 4B). When we performed the same measurements in 1:1 mixture of ethanol and hexane, the force magnitude and the force vs temperature trend was intermediate between what we observed in pure hexane and pure ethanol (Figure 4C).

To rule out interpenetration of the thiol chains as a possible cause for the observed effects, we measured the adhesion force between a bare silicon nitride tip and mica surface. This system also presents interactions between hydrogen-bonding surfaces, albeit in a much less controlled fashion than the thiol modification provides. The adhesion forces measured between this combination of tip and sample in ethanol also increased with the temperature (Figure 5), which rules out thiol entanglement as a potential source of the observed effect. This result is not surprising because thiol SAMs maintain a well-ordered crystalline state at temperatures below 70 °C.[17]

To compare these experimental systems with the system that presents weakly interacting chemical functionalities, we per-

(17) Bain, C. D.; Troughton, E. B.; Tao, Y.-T.; Evall, J.; Whitesides, G. M.; Nuzzo, R. G. *J. Am. Chem. Soc.* **1989**, *111*, 1.

Figure 6. Plots of measured adhesion force as a function of temperature for CH_3-terminated tips and samples measured in (A) ethanol and (B) hexane. Each data point corresponds to an average of 300 individual force vs distance curves.

Table 1. Measured Slopes and Relative Fluctuations of the Adhesion Force vs temperature data shown in Figures 3, 4, 5, 6, and 7

probe	sample	solvent	slope, dF/dT, (pN/K)	average relative fluctuations, $\langle \Delta F/F \rangle$
Au/COOH	Au/COOH	hexane	-2.7 ± 1.4	0.8 ± 0.2
Au/COOH	Au/COOH	ethanol	30.5 ± 4.1	0.3 ± 0.1
Au/COOH	Au/COOH	ethanol/ hexane 1:1	4.8 ± 3.8	0.2 ± 0.05
Au/CH$_3$	Au/CH$_3$	hexane	-0.82 ± 0.32	0.5 ± 0.1
Au/CH$_3$	Au/CH$_3$	ethanol	2.9 ± 0.8	0.3 ± 0.1
Au	Au	ethanol	-0.09 ± 1.75	0.3 ± 0.07
Au	Au	hexane	-3.9 ± 1.55	0.5 ± 0.08
Si$_3$N$_4$	mica	ethanol	3.3 ± 0.4	0.6 ± 0.2

formed similar measurements using the tip and sample terminating with methyl groups. In this system, all of the interactions between the two surfaces are van der Waals and the interactions of the solvent molecules with the surface are very weak. The interactions force measured in ethanol showed an increase with the temperature (Figure 6A), yet the increase was almost an order of magnitude smaller than the increase observed for COOH-terminated functionalities (Table 1). When we switched the solvent to hexane, we again observed a reversal of the trend: the interaction strength decreased with the increase in temperature (Figure 6B).

Finally, to contrast these systems with the system that has no distinct chemical interactions, we studied temperature dependence of the interaction strength between unmodified gold-coated probe and sample, both in ethanol and hexane. The majority of forces in this system result from van der Waals interactions. In addition, bare gold surfaces do not show any specific chemical interactions with ethanol or hexane. When we measured the interaction force between gold surfaces in
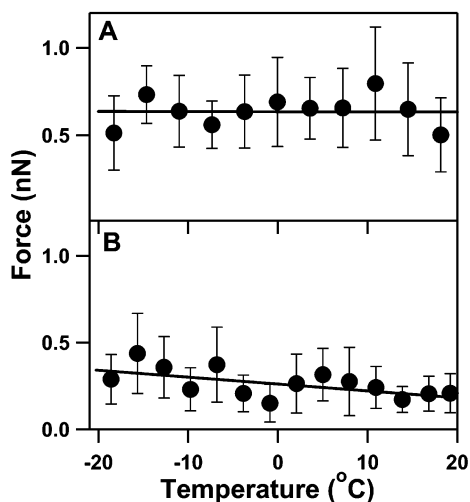
Figure 7. Plots of measured adhesion force as a function of temperature for tips and samples terminated with bare gold measured in (A) ethanol and (B) hexane. Each data point corresponds to an average of 40 individual force vs distance curves.

ethanol we found that it did not show a significant trend over the temperature range that we studied (Figure 7A). When we switched the solvent to hexane, we observed a slight decrease in force value as the temperature increased (Figure 7B).

Our results suggest that the observed experimental trends originate in the interactions of the solvent with the surface. In principle, any surface that interacts strongly with the solvent molecules can induce the formation of a tightly bound first solvent layer. Formation of bound solvent layers at hydrophilic interfaces has been observed previously in AFM[18,19] and surface forces apparatus[20] experiments. These solvent layers are present only when the surfaces are separated; when the surfaces come in contact the solvent molecules are expelled into the bulk fluid (Figure 1B). As the surfaces are pulled apart, reduction in the degrees of freedom for the molecules in these strongly ordered solvent layers should contribute to a large negative entropy change for the unbinding process. Furthermore, as the temperature increases, stronger thermal vibrations of the solvent molecules increase the work required to order these layers. Effectively, the energy barrier increases with temperature, which in turn leads to the observed increase in the adhesion force. Qualitatively, we expect this effect to be strong for polar solvents, which tend to form highly ordered surface layers, and weak for nonpolar solvents. This conclusion is consistent with our observations.

Curiously, our picture for this "solvent ordering effect" parallels a recent finding that strong orientation of water molecules induced by the surface and not strong hydrogen bonding between water molecules is responsible for the "hydrophobic" effect.[21] Moreover, hydrophobic interaction also shows an increase in the interaction strength with the temperature.[1] In effect, we observe behavior that is similar to the interactions of hydrophobic surfaces in water, but in our case

the surfaces are hydrophilic and the solvent is nonaqueous! We also note that the interactions that we observed must be different from the structural solvation forces since these forces are expected to be repulsive for the interactions of hydrophilic surfaces in a polar solvent.[1]

Kinetic Model of Bond Dissociation. We can quantify our phenomenological picture using a kinetic model of chemical-bond rupture based on the Kramers' model of thermally assisted barrier crossing in liquids.[22] Evans and co-workers showed that this model is applicable to the rupture of bonds between ligand–receptor pairs.[5] However, their description concentrated on the effect of the loading rate on the observed unbinding force. We can use the same model to investigate the thermal dependence of the bond strength. Following Evans and Ritchie's description,[9] we consider the unbinding as a first order process of escape from a potential well under the influence of an external loading force. The loading force tilts the potential landscape, effectively reducing the barrier and facilitating the thermally activated escape from the bound state. In this model, the rate of escape from the bound state dP/dt under applied load $f(t)$ obeys first-order kinetics

$$\frac{dP}{dt} = -k_{off}P(t) \tag{1}$$

where P is the population of the bound state and the rate constant k_{off} is inversely proportional to the average bound state survival time. Application of the external load force $f(t)$ will lower the energy barrier and reduce the bound state survival time. Thus the rate constant k_{off} becomes a function of the external force

$$k_{off} = \frac{1}{\tau_D} \exp\left[-\frac{E_0 - f(t)x_\beta}{k_B T}\right] \tag{2}$$

Here E_0 is the activation energy barrier, x_β is the distance between the bound state and the transition state, and τ_D is the characteristic diffusion time of motion in the system. If the external load force changes with time, then the problem becomes a first-order kinetic process with time-dependent rate constant. AFM pull-off force measurements fall in this category because they feature constant rate loading $f(t) = r_f \cdot t$. According to the eq 1, the likelihood of detachment (i.e., probability density $p(t) \equiv dP/dt$) is proportional to rate constant multiplied by the population of the bound state. As the loading force increases, the rate constant increases while the population of the bound state diminishes. Therefore, the probability of detachment will go through a maximum at a certain value of the applied force.[9,23] This value defines the bond strength, $f_{pull-off}$. Interestingly, the kinetic model indicates that (a) pull-off force is a dynamic value determined by the interaction potential and loading conditions, and (b) measured pull-off force distribution is always broadened by the thermal noise even in absence of experimental uncertainties. Evans solved the eqs 1 and 2 to find the position of the detachment probability maximum in the case of a single energy barrier loaded at constant rate and obtained the following

(18) Cleveland, J. P.; Schaffer, T. E.; Hansma, P. K. *Phys. Rev. B–Condensed Matter* **1995**, *52*, R8692–R8695.
(19) Kanda, Y.; Iwasaki, S.; Higashitani, K. *J. Colloid Interface Sci.* **1999**, *216*, 394–400.
(20) Israelachvili, J. *Acc. Chem. Res.* **1987**, *20*, 415–421.
(21) Scatena, L. F.; Brown, M. G.; Richmond, G. L. *Science* **2001**, *292*, 908–912.
(22) Hanggi, P.; Talkner, P.; Borkovec, M. *Rev. Mod. Phys.* **1990**, *62*, 251–341.
(23) Evans, E. *Faraday Discuss.* **1999**, 1–16.

expression for the pull-off force[23]

$$f_{\text{pull-off}} = \frac{k_B T}{x_\beta} \ln\left(\frac{r_f}{r_0}\right) \tag{3}$$

where r_0 is defined as

$$r_0 = \frac{k_B T}{x_\beta} \cdot \frac{1}{\tau_D \exp\left(\frac{E_0}{k_B T}\right)} \tag{4}$$

If we separate the energy barrier into enthalpic and entropic components, then $E_0 = \Delta H - T\Delta S$, and substitute eq 4 into eq 3, we can then represent eq 3 in a much more revealing form

$$f_{\text{pull-off}} = \frac{\Delta H}{x_\beta} - \frac{\Delta S}{x_\beta} T - \frac{k_B T}{x_\beta} \ln\left[\frac{k_B T}{r_f \tau_D x_\beta}\right] \tag{5}$$

The first two terms in eq 5 describe the enthalpic and the entropic contribution to the bond strength and the third (kinetic) term describes the contribution of thermal motion to the bond strength. In other words, the first two components describe the true energy-barrier contribution and the always negative[24] third component describes the "thermal weakening" of a bond caused by the thermal fluctuations helping the system to get over the activation barrier.

We can rationalize our experimental observations by considering the thermal dependence of the second and third terms of eq 5. The third term in the eq 5 ("thermal weakening") always increases in magnitude as the temperature increases, leading to the overall decrease in the observed force, in full agreement with the intuitive picture of bond "loosening". The entropic term can lead to either increase or decrease in the overall interaction force depending on the sign on the entropy change for the unbinding process. We expect the solvent entropy contribution to be negative for the probe-surface interactions in fluids due to the ordering of the solvent in the vicinity of the surfaces upon their separation. Therefore, the entropic term will tend to increase the overall interaction force with the temperature increase. The relative magnitude of the entropic and the kinetic terms then defines two regimes of bond rupture: (a) thermally dominated kinetics where the kinetic weakening leads to decrease in the observed bond strength with the increase in temperature and (b) barrier-dominated kinetics where the entropic term overwhelms the kinetic term and leads to an increase in interaction strength with increase in temperature. This prediction is consistent with our experiments: in a polar solvent such as ethanol, which forms ordered layers, the entropic contribution from ethanol molecules overwhelmed the contribution due to thermal fluctuations and the interaction force increased with temperature. Ethanol interacts stronger with the hydrophilic COOH-terminated monolayer than with the CH_3-terminated monolayer, therefore COOH-terminated monolayers show a much stronger increase in the interaction force with the

temperature. When we switched the solvent to hexane, a nonpolar solvent, the magnitude of the entropic term decreased. Consequently, the unbinding regime switched to thermally dominated kinetics, causing the observed inversion in the force vs temperature trend.

Further analysis of the eq 5 indicates that the entropic regime of unbinding must exist only in the limited range of temperatures. As the temperature increases further, kinetic term which increases as $T \cdot lnT$ will always overwhelm the entropic term which increases only linearly. This crossover point simply corresponds to the situation when the thermal motion becomes so strong that it overwhelms molecular ordering in the solvent layers induced by the surface.

Measured slopes of the force vs temperature data on the Figure 4 can provide a consistency check for our model. For pure thermally dominated kinetics when the contribution from the entropic term is negligible, the slope of the force vs temperature data is given by the derivative of the kinetic term with respect to temperature, and thus must be equal to $-k_B/x_\beta(\ln(k_B T/x_\beta r_f \tau_D) + 1)$. We calculated the slope of -1.6 pN/K for our experiments,[25] which is close to the value of -2.7 ± 1.4 pN/K that we observed for the interactions of COOH-terminated surfaces in hexane (Table 1). Additionally, if we assume that the entropic term dominates the kinetics for the interactions COOH-terminated surfaces in ethanol, then we can use the slope of the force vs temperature data (Table 1) to estimate the entropic change associated with the tip-sample interactions to be 40.3×10^{-21} J/K. This entropy change normalized to one interacting functional group provides a more meaningful value. Previous work reported that interaction of COOH-terminated surfaces in ethanol involves ~20 surface functional groups.[11] Therefore, we estimate the entropy change associated with the area of one COOH functional group in the SAM to be $2.0 \cdot 10^{-22}$ J/K. This value is more than an order of magnitude higher than the value of k_B, therefore, the thermal motion is indeed insufficient to break the ordering of the solvent molecules at the interface. Recently, Schumakovitch et al. measured binding forces between short complementary DNA oligonucleotides as a function of temperature and reported a large thermal dependence of values of interaction potential width x_β, which they also attributed to entropic effects.[26] However, we note that the breakup of DNA duplex is always associated with large conformational changes,[2,27,28] whereas rigid self-assembled monolayers used in our experiments make such changes rather unlikely. In addition, our system presents a much simpler interaction than the system used by Schumakovitch et al., therefore, we cannot justify a direct comparison between them.

(24) The kinetic term is always negative if we assume that the loading rate is slow compared to the diffusion time of motion in the system. Mathematically, it means that the loading rate r_f must satisfy the following condition: $r_f \leq k_B T/x_\beta \tau_D$. If the system is loaded faster than this threshold rate, then the system cannot reach thermal equilibrium and the kinetic model is no longer applicable. An order-of-magnitude estimate using $x_\beta = 1$ Å and $\tau_D = 10^{-10}$ s yields the cutoff value for the loading rate $r_f = 4 \times 10^8$ nN/s, which is about 5–6 orders of magnitude higher than the rate typically used in AFM measurements.

(25) In the absence of better literature values, we used order of magnitude estimates for x_β and τ_D. We took an estimate for the τ_D value from ref 23, which states that attempt frequency for overdamped transitions in liquids are typically 3 orders of magnitude smaller than the resonant frequencies of bond excitation. Assuming a typical resonant bond excitation time of 10^{-13} s, we arrive at the τ_D estimate of 10^{-10} s. We took $x_\beta = 1$ Å as an order of magnitude estimate of a typical intermolecular distance. However, after this paper was submitted for the review, we determined the value for x_β experimentally by measuring the adhesion force as a function of loading rate.[32] All of the estimates in the paper are based on this experimental value of $x_\beta = 1.32$ Å.

(26) Schumakovitch, I.; Grange, W.; Strunz, T.; Bertoncini, P.; Guntherodt, H. J.; Hegner, M. *Biophys. J.* **2002**, *82*, 517–521.

(27) Smith, S. B.; Cui, Y.; Bustamante, C. *Science* **1996**, *271*, 795.

(28) Noy, A.; Vezenov, D.; Kayyem, J.; Meade, T.; Lieber, C. *Chem. Biol.* **1997**, *4*, 519–527.

Force fluctuations can provide additional information about the processes occurring in our system. Large fluctuations in the measured force values that we observed can be associated either with the thermal motion or with the fluctuations in contact area.[29] Significantly, these two sources should lead to very different fluctuation magnitudes in our experiments. The kinetic model[9] predicts that thermal motion should result in force fluctuations on the order of $k_B T/x_\beta$, independent of both the contact area size and the magnitude of the pull-off force (assuming that x_β is independent of these quantities). For the interactions of carboxyl-terminated SAMs in ethanol this model predicts relative fluctuations $\Delta F/F$ to be on the order of 0.02, which is about an order of magnitude lower than our experimental value of 0.3 (Table 1). Alternatively, if the force fluctuations are caused by the fluctuations in the tip−sample contact area and N identical bonds comprise the interaction, then we expect the average relative fluctuations to scale as $1/\sqrt{N}$. For the interactions between COOH-terminated groups in ethanol (if all ∼20 groups in the tip−sample contact area interact with one another) we should expect the magnitude of the fluctuations to be about 0.2 of the total force, which is reasonably close to our experimental value of 0.3 (Table 1). The discrepancy between our experimental value and the theoretical estimate might be explained if we consider that not all the functional groups in the contact area participate in the interaction, increasing the relative binding force fluctuations even further. Thus, we conclude that fluctuations in the number of the interacting functional groups likely cause the large fluctuations in the binding force observed in our experiments.

Last, we will consider the implications of our results to the problem of measuring single-bond strength in fluids. We have shown that the surrounding medium can completely obstruct true chemical interactions due to the entropic effects. To obtain a true measurement of chemical bond strength, we will need to tune the medium carefully to eliminate the solvent contribution as much as possible.[30] Alternatively, because the entropic term is sensitive to the probe-sample contact area, we may try to reduce the size of the probe to achieve the same goal. The entropic contribution associated with the solvent ordering must scale with tip−sample contact area. In contrast, the kinetic term is independent of the contact area. Therefore, as the size of the probe shrinks, we expect a crossover from the solvent-dominated unbinding regime to the kinetic regime that will reveal the true strength of intermolecular interactions. For example, functionalized carbon nanotube AFM probes[31] will likely operate in the kinetic regime. Regardless of the chosen approach, a simple extrapolation of the results of the large contact-area, multi-bond interaction measurements to the single-bond interaction regime is likely incorrect. Instead, only a careful consideration of different unbinding regimes and different contributions to the interaction strength couples with a careful choice of the experimental conditions will bridge the gap between these two types of measurements.

Conclusions

We used variable temperature chemical force microscopy to demonstrate that the interactions measured in an atomic force microscopy experiment can occur in two distinct regimes: (a) a thermodynamic regime, dominated by solvent entropy contribution to the energy barrier, and (b) a kinetic regime, dominated by thermal fluctuations. We showed that the interactions between hydrophilic chemical functional groups in ethanol occur in the thermodynamic regime, as evidenced by the increase in the interaction force with temperature. We attributed the origin of this entropic barrier to the ordering of the ethanol molecules at the interface. When we measured the same interactions in hexane, the binding switched to the kinetic regime, reversing the force vs temperature trend. For the probe and sample surfaces terminating with bare gold the solvent-surface interaction was too weak to contribute to a significant entropic barrier and shift the unbinding into the kinetic regime.

Our results carry broad implications for understanding intermolecular interactions and interfacial phenomena at the nanoscale. Researchers often assume that, with the exception of hydrophobic interactions, the solvent medium is a secondary factor, whereas the effective energy barrier is structured purely by intermolecular potentials. Yet, we showed that a solvent entropy effect similar to the hydrophobic effect is dominating the interactions between hydrophilic surfaces in a polar non-aqueous solvent. Our data indicate that hydrophobic interaction mechanism is not uniquely confined to water. Instead, entropic barriers shaped by the interactions of solvent molecules with the surface exist in a much wider variety of systems. Therefore, the role of the solvent in structuring the energy barriers encountered in nanoscale interactions in condensed phases must be always carefully considered. Only then will a truthful picture of the intermolecular potentials emerge.

JA026865P

(29) Williams, J. M.; Han, T.; Beebe, T. P., Jr. *Langmuir* **1996**, *12*, 1291−1295.
(30) Skulason, H.; Frisbie, C. D. *J. Am. Chem. Soc.* **2000**, *122*, 9750−9760.
(31) Wong, S. S.; Joselevich, E.; Woolley, A. T.; Cheung, C. L.; Lieber, C. M. *Nature* **1998**, *394*, 52−55.
(32) Zepeda, S.; Yeh, Y.; Noy, A. *Langmuir* **2002**, accepted.